Comparisons on the Differences in Numerical Modelling Methods between Pre-bored Pressuremeter and Self-bored Pressuremeter

F. Phangkawira[1], D. E. L. Ong[1] and C. S. Choo[1]

[1]*Research Centre for Sustainable Technologies, Swinburne University of Technology Sarawak Campus,*
Kuching, Sarawak, Malaysia
E-mail: fphangkawira@swinburne.edu.my

ABSTRACT: Numerical modelling has proved its versatility in assisting to solve many engineering problems. It has also opened many opportunities for interpretations of material testing which cannot be obtained by the means of analytical approaches alone. Numerical approach is one of the favourable alternatives in interpreting effective strength parameters of highly fractured and weathered rocks from pressuremeter tests. While there are many different types of pressuremeters nowadays, with different designs and tests procedures, the numerical modelling process might not be the same for every instrument. This paper serves to review the difference between two of the most common types of pressuremeters, namely pre-bored pressuremeters (PBPM) and self-boring pressuremeters (SBPM). The two instruments were compared in terms of their physical designs, working mechanisms, test procedure and most subsequently, the impact of their testing characteristics on the numerical modelling process.

KEYWORDS: Pressuremeter test, Self-boring pressuremeter, Menard pressuremeter, Numerical modelling

1   INTRODUCTION

A pressuremeter test (PMT) is an in-situ test that measures the physical characteristics of a soil or rock section using an inflatable cylindrical probe. It is conducted by lowering the probe into a borehole to the depth of the test section. The probe is subsequently inflated, thus pressurising the surrounding geology. Stresses and strains around the borehole wall are measured through transducers that are installed inside the inflatable probe. From these measurements, a pressuremeter curve in the form of a stress-strain plot can be generated to analyse the physical characteristics of the tested geology (Briaud, 1992). Currently, there are many different types of pressuremeter available in the market, e.g. pre-bored pressuremeter (PBPM), self-bored pressuremeter (SBPM), cone pressuremeter (CPM) and pushed Shelby tube pressuremeter (PSPM). However, this paper only discusses on the characteristics of PBPM and SBPM as there is a significant difference in the installation procedures for these two instruments. As a result, its interpretation methods and numerical modelling may not be identical. By comparing their overall testing procedures, one may potentially gain better insights on how the differences in the installation method may affect the numerical modelling process of a pressuremeter test.

1.1   A brief history of pressuremeter

The first design of pressuremeter is the PBPM, which was initially developed by Kogler in Germany, 1933. However, his idea was not invested further until a French man called Louis Menard built the fully operational device in 1955 (Gambin, 1990). The instrument soon gained popularity as different types of pressuremeters started to emerge in other countries. For example, Elastmeter 100, which is a PBPM built by Suyama, Imai and Ohya from Oyo Corporation in 1966 and SBPM by Wroth and Hughes in England, 1971 (Wroth, 1982).

1.2   PMT application in various geology

PMT has been used to test various types of geology, ranging from soft soils to rocks. Clarke (1995) provided a general summary of the applicability of PBPM and SBPM for different geology in Table 1, where A is very feasible, B is feasible, C is moderately feasible and N is not feasible.

Meanwhile, several authors have studied on the methods to interpret PMT results in cohesive soils (Baguelin et al., 1978;

Gibson and Anderson, 1961; Marsland and Randolph, 1977; Palmer, 1972), granular soils (Hughes et al., 1977; Ladanyi, 1963) and rocks, specifically weak rocks (Clarke and Smith, 1992; Dafni, 2013; Haberfield and Johnston, 1989). The theoretical background behind these methods is based on the cavity expansion theory of an infinitely long cylindrical expansion in an infinite soil mass (Vesic, 1972; Yu, 2000). It is also important to note that the analysis for cohesive and granular soils assumes undrained and drained conditions respectively.

Table 1 The applicability of SBPM and PBPM on various geology (Clarke, 1995).

Geology	SBPM	PBPM
Soft Clay	A	A
Stiff Clay	A	A
Loose Sand	A	B (with support)
Dense Sand	B	B (with support)
Gravels	N	C by driving
Weak Rock	B	A
Strong Rock	N	A

Since pressuremeter was initially built for soil testing, it is expected that the interpretation of PMTs performed in soils would be better established than those performed in rocks. This is because soil behaviour is better understood as compared to that of rocks. Also, the availability of well-established laboratory tests for soils may serve as benchmarks, which helps to raise confidence in the development of PMT interpretation methods for soils.

When dealing with rocks however, PMT interpretations can be more complicated. This might be due to the anisotropy of rock masses which give rise to challenges in the development of reliable interpretation methods. For example, some of the physical features in rocks, such as joints, weathering and dip angles, affect their strength and stiffness. In some cases, especially in highly fractured and weathered rocks, it is even harder to develop analytical approaches to interpret PMT results.

Since most of the current interpretation methods are applicable to soils in undrained conditions (Briaud, 1992; Gibson and Anderson, 1961; Palmer, 1972), the established methods should be used with caution when interpreting the PMT results from tests performed on rocks. As a result, the development of PMT interpretation in highly fractured and weathered rocks becomes challenging. This has led to the use of numerical modelling in

facilitating the analysis of PMTs performed in rocks (Fawaz et al., 2002; Haberfield and Johnston, 1989; Isik et al., 2008).

1.3 Numerical approach for PMT interpretation

The general idea of numerical modelling in geotechnical field is to create a simulation of a real-life phenomenon in order to study or predict the behaviour of the geology. Modelling a PMT usually assists researchers in performing interpretations which cannot be done by analytical approaches alone. This is because many of them depend on theoretical assumptions which sometimes generate a level of over-idealisation. An example is shown in the works of Haberfield and Johnston (1989) that used numerical approach to interpret the effective strength parameters of weak rocks using PMT. One of the reasons why they resorted to this approach is because most of the established analytical interpretation assumes undrained conditions, which are not always the case for fractured rocks since there is a high chance that water can seep through the joints. This observation provided the basis for the current study. In this study, numerical modelling of PBPM test is done using the Hardening Soil Model (Schanz et al., 1999) that is available in a numerical modelling software called PLAXIS 3D (Plaxis, 2013).

1.4 Aim and objectives

The aim of this paper is to generate a comparison between the PBPM test and SBPM test. Detailed descriptions of each instrument are presented to review the important differences between the two tests in terms of their instrument designs, test procedures and results. Due to these, the numerical modelling techniques for each test might have their own distinctions. Therefore, the difference between the modelling process for PBPM test and SBPM test is also compared. In this study, the numerical modelling of PBPM tests via PLAXIS 3D is compared against those for SBPM tests from various literatures.

2 PRE-BORED PRESSUREMETER (PBPM)

2.1 Instrument description

There are essentially three components of a PBPM, namely a control unit, a tubing system and an inflatable probe. The control unit contains valves and switches used to control the expansion of the inflatable probe through the tubing system. In more conventional designs of pressuremeter, measurements are directly read from the analogue pressure gauge installed in the control unit, as shown in Figure 1.

Figure 1 The control unit of the classic Menard pre-bored pressuremeter.

Alternatively, modern designs of control units allow measurements to be taken digitally via a data logger. An example of pressuremeter which adopts this system is Oyo Elastmeter (Figure 2).

Figure 2 Oyo Elastmeter with digital data logger.

Generally, there are two types of PBPM probes, namely single-celled probes and triple-celled probes. Early pressuremeter designs normally use triple-celled probe, which consist of a measuring cell and two guard cells. The measuring cell is a unit in where transducers are installed for measurements of stresses and deformations. These sensors measure pressure changes and volumetric deformation of the cell. The guard cells help to prevent the effects of curvature that exist at the top and bottom ends of the probe from reducing the accuracy of the deformation measurements, while at the same time preventing the measuring cell from expanding vertically. A single-celled probe is much simpler as it consists of only one measuring cell. The effects of curvature at the probe ends are mitigated through the use of a longer measuring cell in the probe. Figure 3 shows the schematics of a triple-celled and a single-celled probe.
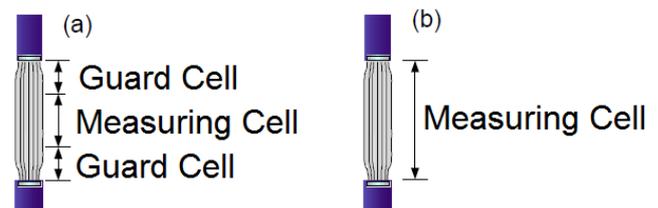

Figure 3 Schematics of (a) triple-celled probe and (b) single-celled probe.

2.2 Testing procedure

A pressuremeter test is conducted by inserting the inflatable probe into a borehole to a required depth within a tested geology and then expanding it to measure the changes in pressure and volume in the probe. For a PBPM, a borehole has to be drilled before the insertion of the probe. ASTM D4719 (2000) provides a comprehensive procedure for the PBPM test, which is summarised in this paper, hereinafter.

Prior to the testing, calibration exercises are done to compensate for the losses in pressure and volume measurements due to the stiffness and the compressibility of the probe membrane, respectively. By doing so, the measurements taken during the test can be corrected to obtain the true measurements of the stresses and deformation in the surrounding geology. Pressure loss calibration is performed by inflating the probe at ground level in atmospheric pressure. Meanwhile, volume loss calibration is done by inflating the probe within a heavy duty steel casing.

After the calibration is done, a borehole is drilled as an access channel to lower the probe down to the test depth. The diameter of the borehole is made with reasonable tolerance to ensure that it is not too small or too large for the probe. Specifications regarding the measurements of the borehole diameter are further explained in

ASTM D4719 (2000). It is also important to ensure that the drilling process is done carefully to minimise disturbance to the borehole wall, which may alter the test results significantly.

After the borehole is prepared, the probe is lowered to the required depth for testing. The test can either be pressure-controlled or deformation-controlled. A pressure-controlled test is basically done by regulating the pressure increment as the corresponding deformations are measured, while a deformation-controlled test works the opposite. In this study, the PBPM tests were done as pressure-controlled tests. A pressuremeter test is usually performed in a relatively short time to prevent excessive groundwater seepage.

2.3   Typical results and interpretation

Once the test is complete, the pressure and deformation measurements are corrected using the calibration data through a simple calculation specified in ASTM D4719 (2000). The corrected pressure, p_c is plotted against corrected volume, V_c to produce a plot similar to Figure 4.
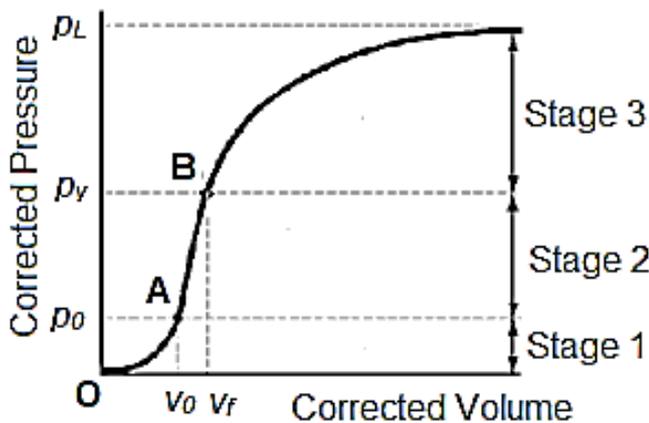
Figure 4 Typical pressuremeter curve obtained using pre-bored pressuremeters (PBPM).

Throughout the test, the surrounding geology experiences three deformation stages:

- Stage 1 – Initiation Stage
- Stage 2 – Pseudo-elastic Stage
- Stage 3 – Plastic Stage.

Stage 1 begins after the geology surrounding the borehole cavity experiences stress relief from initial in-situ stresses p_0 to point O in Figure 4. The in-situ stresses are then restored back to point A, by the applied pressure from the pressuremeter probe.

Stage 2 starts as a linear stress-strain progression of PMT curve beyond point A towards point B. The linear progression implies that the tested geology deforms elastically at a constant rate of pressure increment. Hence, a pressuremeter modulus E_{PMT} can be interpreted from this stage. The calculation for E_{PMT} as given by ASTM D4719 (2000) is presented in Eq. (1).

$$E_{PMT} = 2(1 + v)(V_0 + V_m)\frac{\Delta P}{\Delta V} \qquad (1)$$

where v is Poisson's ratio, V_0 is the uninflated probe volume, V_m is the midpoint of the corrected volume reading at Stage 2 and $\Delta P/\Delta V$ is the gradient of the linear stress-strain progression after p_0.

Stage 3 begins at point B, which is at the yield pressure, p_y. At this stage, the tested geology undergoes plastic deformation to a perfectly plastic state as indicated by the continued deformation at a constant applied pressure. This pressure is labelled as limit pressure, p_L. Several authors have developed methods to interpret undrained shear strength, c_u from this stage of PMT curve (Gibson and Anderson, 1961; Marsland and Randolph, 1977).

3   SELF-BORED PRESSUREMETER (SBPM)

3.1   Instrument description

SBPM probes are generally similar to the PBPM probes. Most of them use single-celled probes, which haves been described previously. SBPM probes are distinct from PBPM probes by the inclusion of a self-boring head at the bottom of the SBPM probe, as shown in Figure 5.
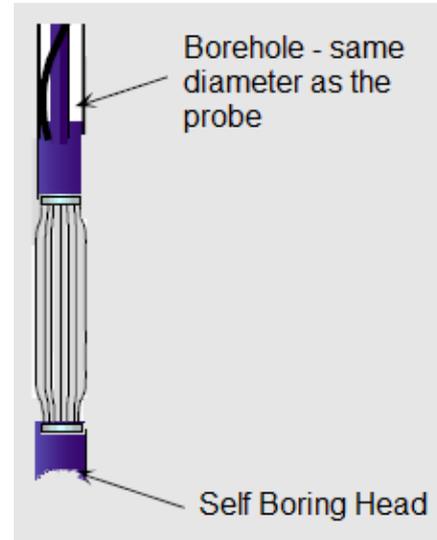
Figure 5 Schematics of SBPM probe.

This head serves as a cutter face that allows for borehole excavation to occur simultaneously as the pressuremeter probe is lowered down to the test depth. As a result, the diameter of the borehole is usually similar to that of the probe. Under ideal conditions, this prevents the stress relief of the surrounding geology from happening.

Nowadays, there are two mechanisms of self-boring head that are generally implemented for SBPM probes, i.e. the cutter face mechanism and the jetting mechanism (Benoit, 1995). The cutter face mechanism is a technology used by Wroth and Hughes (1973) in the earlier iterations of the SBPM developed by Cambridge University. It functions as a normal cutting tool which crushes the underlying geomaterial into smaller pieces, after which the crushed spoils are transported upwards and away from the cutter face. This mechanism is highly applicable for most soils and weak rocks, but is usually very slow and inefficient. The jetting mechanism, developed by Hughes et al. (1984), shows more sophistication as it utilises compressed water to cut the geomaterials, which is subsequently flushed upwards for removal.

3.2   Testing procedure

The SBPM test adopts the same calibration procedures as the PBPM tests, which have been explained previously. It is different however, when it comes to installing the probe to its required test depth. Clarke and Smith, (1992) provided a step-by-step installation procedure for SBPM test in weak rocks. The sequence is summarised as follows:

1. A borehole is created using the common core drilling technique as the access point for the probe. The borehole is advanced to approximately 1 metre above the designated test depth.
2. The instrument is lowered down to the base of the borehole to continue the remaining excavation down to the required test depth.
3. The test is performed. Similar to the PBPM, the test can be a pressure-controlled or deformation-controlled.

The borehole excavation in the first step is done to reduce the time it takes for the probe to reach its test depth. This is very useful especially for tests conducted at deep sections. Unlike the PBPM test, the excavation in step 1 only reaches down to a safe level above the pre-determined test depth. Therefore, the drilling activity does not compromise the integrity of the undisturbed test section.

3.3 Typical results and interpretation

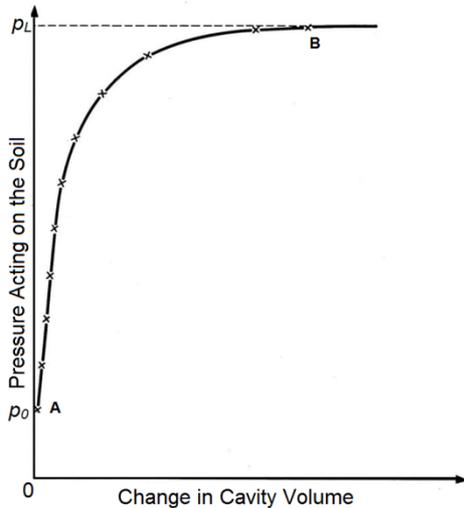Figure 6 shows the PMT curve obtained using SBPM.

Figure 6 Typical pressuremeter curve obtained using self-boring pressuremeters (SBPM).

As compared to typical PBPM test curves, SBPM test curves start from point A at the horizontal in-situ stress, p_0 when there is no deformation recorded. Therefore, the Initiation Stage of the PBPM test curves does not exist in the SBPM test curves. This is due to the simultaneous borehole excavation and probe lowering processes which significantly reduce the degree of stress relief from the surrounding geology. Also, since the borehole and the probe are of the same diameter, it can be said that the probe "replaces" the excavated geology within the borehole. Hence, it experiences the horizontal in-situ stresses p_0 of the surrounding geology, which is recorded at the beginning of the SBPM test curve. The remaining sections of the curve are identical to that of PBPM test, which have been explained earlier.

In comparison, the pressuremeter curves of the two instruments are similar. The only difference lies in the absence of the Initiation Stage in SBPM test curve. Therefore, interpretation methods that are used for PBPM test are also applicable for SBPM test (Yu, 1994). This is because they are based on either the Pseudo-elastic Stage or the Plastic Stage of the pressuremeter curve.

3.4 Numerical modelling methods

The numerical modelling of a SBPM test is generally considered to be simple. Several authors have performed its numerical modelling using 2D modelling software (Bahar and Belhassani, 2012; Jang et al., 2003). The construction of a model for an SBPM test begins with the definition of initial geostatic conditions according to the real test conditions. This includes the determination of the appropriate parameters for each type of geomaterial in the modelled geology, the depth of groundwater table, K_0 conditions and the model boundary conditions. The next stage is the application of a radial stress against a portion of geology at the required test depth.

4 NUMERICAL MODELLING OF PBPM TEST

With the same purpose outlined in Section 1.3, numerical modelling of PBPM tests was based on two real tests (namely BH-A and BH-

B) that were conducted in highly weathered and fractured phyllite. This was done in order to interpret the effective strength parameters of such geology from PBPM test curve, which may potentially be useful for many geotechnical analyses that involve effective stress conditions. In this study, the Hardening Soil Model (HSM) was used to model the highly weathered and fractured phyllite. Since this study considered the remaining soil strata above the phyllite layer only as overburden, for simplification purposes, the Mohr-Coulomb model was used to define their mechanical characteristics.

4.1 The Hardening Soil Model

The Hardening Soil Model (HSM) is a hyperbolic constitutive model which takes into account the stress dependent stiffness of a material. Additionally, since it was first made as an extension of the Mohr-Coulomb (MC) failure criterion (Nordal, 1999), its effective strength envelope is controlled by effective MC strength parameters, i.e. cohesion, *c'* and internal friction angle *φ'*. The formulation of this model is further detailed by Schanz et al. (1999). In this model, there are 10 input parameters, which are listed in Table 2.

Table 2 Input parameters for the Hardening Soil Model.

Input Parameter	Description
E_{50}^{ref}	Reference secant modulus from drained triaxial test
E_{eod}^{ref}	Reference oedometer modulus
E_{ur}^{ref}	Reference unload-reload modulus
c' (kPa)	Effective cohesion
m	Stress-dependent power
φ' (°)	Internal friction angle
ψ' (°)	Dilatancy angle
R_f	Failure ratio
K_0^{nc}	Coefficient of earth pressure at rest under normal consolidated condition (default setting: $1 - \sin\varphi'$)
v_{ur}	Unload/reload poisson's ratio (default = 0.2)

4.2 Modelling process

The numerical modelling of PBPM test in PLAXIS 3D started with the definition of geology. The thickness and the mechanical properties of relevant soil and rock layers were first defined accordingly to simulate the real geological conditions. A cylindrical volume was then created at the centre of the modelled geology to represent the borehole. The cylinder was constructed using the same diameter as the borehole and extruded to the same depth as the real PBPM test. Finally, a positive perpendicular surface load was introduced at the portion of the borehole wall where the pressuremeter probe is located (at the test depth). The geometry of the PBPM test model is shown in Figure 7.
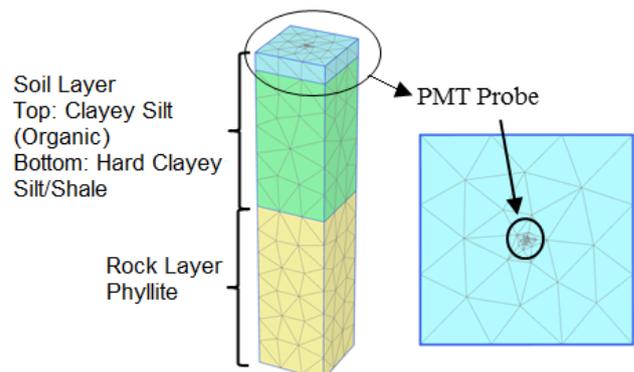

Figure 7 3D model of PBPM test.

Once the essential model components have been created and meshed accordingly, a sequence of construction stages is defined to simulate the procedure of the PBPM test.

Three stages were set in the numerical modelling of PBPM test:

- Stage 1 – Establishment of initial geostatic stresses.
- Stage 2 – Borehole Excavation
- Stage 3 – Activation of applied pressure at test depth.

Stage 1 was automatically generated as a starting point for all consequent construction stages. In this phase, the initial stress conditions were generated based on the input values for material unit weight, groundwater table, K_0 conditions and boundary fixities. The unit weight of relevant soil/rock layers and groundwater levels were set accordingly to portray the in-situ conditions and the default boundary configurations were used for all models.

Stage 2 involved deactivating the constructed cylindrical soil volumes to create a borehole cavity. By doing so, the model read the action as a removal of soil volume, which is analogous to an excavation.

Stage 3 consisted of the activation of positive radial pressure against the borehole wall at the test depth. The positive sign convention of the applied radial pressure indicates an outward pressure away from the borehole cavity, which led to the simulation of cavity expansion created by the inflating pressuremeter probe.

4.3 Determination of HSM parameters

In order to model an accurate behaviour of highly fractured and weathered phyllite bedrock, an appropriate set of HSM input parameters were required. For all models in this study, the HSM parameters for the bedrock were optimised to produce stress-strain curves which would produce lines of "best-fit" to the stress-strain curves produced from in-situ pressuremeter tests. The optimised HSM parameters are shown in Table 3.

Table 3 Optimised HSM parameters for phyllite bedrock.

Pressuremeter Test Location	BH-A	BH-B
E_{50}^{ref} (MPa)	109	251
E_{eod}^{ref} (MPa)	109	251
E_{ur}^{ref} (MPa)	326	753
m	0.5	0.5
c' (kPa)	2400	2700
φ' (°)	39.2	39.2
ψ' (°)	0	0
R_f	0.9	0.9
v_{ur}	0.2	0.2
K_0^{nc}	0.36	0.36

To allow for a fit between the numerical results and the field test results, measurements from the in-situ pressuremeter tests were modified. The reasons and details of the modification are discussed, hereinafter.

5 RESULTS AND DISCUSSION

5.1 Numerical modelling results

A comparison of the PBPM test curves generated from the numerical modelling against those produced from in-situ pressuremeter tests is presented in Figure 8. The figure shows that, unlike real PMT data, the test curves generated from the numerical modelling process do not show the Initiation stage despite the borehole excavation process being included in the modelling sequence. This might be caused by the nature of HSM in modelling a PMT curve. The parameter E_{50} of HSM governs the secant gradient of the hyperbolic stress-strain curve which is comparable to the Pseudo-elastic stage and the Plastic stage. Janin et al. (2015) suggested that the input value for E_{50} should be the Young's

Modulus obtained from the pressuremeter test. This parameter is related to E_{ur}, which is the unload-reload modulus that controls the gradient of the Initiation Stage. This is because the stress path in the Initiation stage is still in the elastic zone of HSM (Schanz et al., 1999). In this model, E_{ur} should be at least twice the magnitude of E_{50}. This is to fulfil the shear hardening equation in HSM which is given as

$$2\varepsilon_1^p = \frac{q_a(2-R_f)}{E_{50}} \frac{q}{q_a - q} - \frac{2q}{E_{ur}} \tag{2}$$

where ε_1^p is the plastic strain, q is the deviatoric stress and q_a is the asymptotic shear strength.
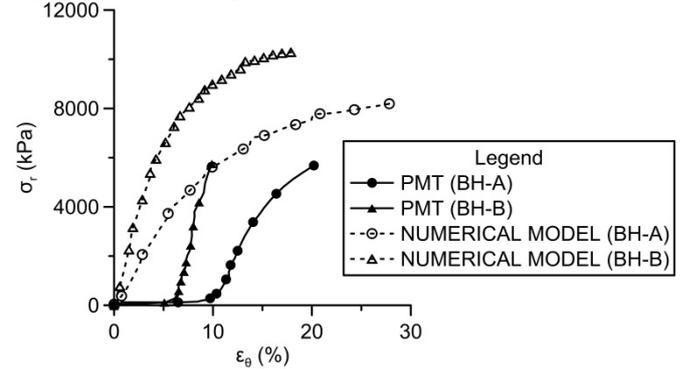
Figure 8 Comparison between the numerical modelling and the real PBPM test curve.

In small-strain cases, this equation would calculate to a negative value of ε_1^p for any values of E_{ur} that is less than twice of E_{50}. This is invalid because it indicates an opposite direction of strain in response to the applied deviator stress, q. As a result, the modelling of PMT using the HSM requires a compromise in modelling either the Initiation stage or the Pseudo-elastic stage. This is because, to model the gentle slope in the Initiation stage would require a low E_{ur} value, while modelling the steep gradient in the Pseudo-elastic stage requires a high E_{50} value.

Due to the reasons above, the PBPM test curves were modified to exclude the Initiation Stage so that they can be compared against the modelled curves. Briaud (1992) suggested that the portion of the PMT curve at stresses less than p_0, i.e. the Initiation stage can be excluded so that only the Pseudo-elastic stage and the Plastic stage is shown. This is done by changing the deformation axes from the Corrected Volume, V_c readings into the relative change in the probe radius ($\Delta R/R_0$) and then re-zeroing the axis at the corresponding $\Delta R/R_0$ value at p_0. The modified pressuremeter test curves and their comparison with the numerical modelling results are presented in Figure 9.
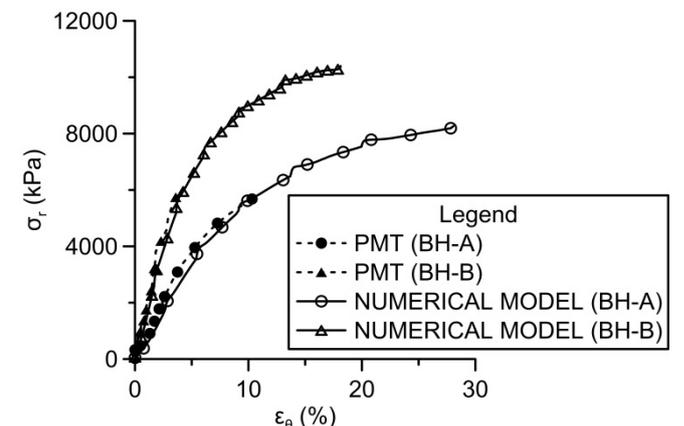
Figure 9 Comparison between the numerical modelling and the modified PBPM test curve.

This technique of modifying the in-situ pressuremeter test curves allowed for the development of suitable HSM parameters, as shown in Table 3.

5.2 Comparison with numerical models of SBPM test

As compared to that of PBPM test, the modelling process for SBPM test does not require a construction stage for borehole excavation. As a result, the numerical models of SBPM test will automatically produce a stress-strain curve that starts from p_0, similar to the real test. This enables a direct comparison between the modelled and the real test curve, which is more convenient since the absence of the Initiation stage in the real SBPM test curve removes the need for the modification process that is used in the methods for PBPM test.

6 CONCLUSION

In terms of instrument design, pre-bored pressuremeters (PBPM) and self-bored pressuremeters (SBPM) has exhibited many similarities, except for the self-boring head component in the SBPM. This component allows the probe to be lowered almost at the same time as the excavation of the borehole, which significantly reduces the stress relief of the surrounding borehole walls. As a result, the typical SBPM test curve does not have the Initiation Stage that is shown in PBPM test curve. Instead, the curve starts at a pressure reading above zero, which is evaluated as the horizontal in-situ stress, p_0. The measurement for p_0 using SBPM is arguably more accurate than PBPM due to the significantly less disturbance caused by the borehole excavation process. On the other hand, the usage of SBPM is not as wide as PBPM. This might be caused by the incompatibility of the boring head with certain types of geology (Clarke, 1995).

The different designs and test procedures of PBPMs and SBPMs have also shown a noticeable impact on their respective modelling processes. A numerical approach to interpret a PBPM test would require a modification on the real test curve as evidently shown in this paper to exclude the Initiation stage, i.e. the portion of the curve at stresses below p_0. Meanwhile, in the case of SBPM test, this process is unnecessary as the stage is not presented in the SBPM test curve. This is caused by the self-boring mechanism in the instrument which almost eliminates the stress relief of the geology surrounding the borehole.

7 REFERENCES

ASTM (2000). "Standard test methods for prebored pressuremeter testing in soils." D4719-07, West Conshohocken, PA.

Baguelin, F., Jezequel, J. F. and Shields, D. H. (1978). The Pressuremeter and Foundation Engineering, Trans Tech Publications, Aedermannsdorf, Switzerland.

Bahar, R. and Belhassani, O. (2012). "Numerical analysis of a cyclic pressuremeter test." Proceedings of the Fifteenth World Conference on Earthquake Engineering, Lisbon, Portugal.

Benoit, J. (1995), "Advances in pressuremeter technology with specific reference to clays." in G Ballivy (ed.), Proceedings of the Fourth International Symposium on Pressuremeter, Quebec, Canada, 125-139.

Briaud, J. L. (1992). The Pressuremeter, A.A. Balkema, Rotterdam.

Clarke, B. G. (1995). Pressuremeters in Geotechnical Design, Blackie Academic & Professional, London.

Clarke, B. G. and Smith, A. (1992). "Self-boring pressuremeter tests in weak rocks." Construction and Building Materials, 6(2), 91-96.

Dafni, J. (2013). "The Analysis of Weak Rock Using the Pressuremeter", PhD thesis, University of Washington.

Fawaz, A., Boulon, M. and Flavigny, E. (2002). "Parameters deduced from the pressuremeter test." Canadian Geotechnical Journal, 39(6), 1333-40.

Gambin, M. (1990). "The history of pressuremeter practice in France." Proceedings of the Third International Symposium on Pressuremeters, Oxford, 5-24.

Gibson, R. E. and Anderson, W. F. (1961). "In-situ measurement of soil properties with the pressuremeter." Civil Engineering and Public Works Review, 56(658), 615-618.

Haberfield, C. and Johnston, I. (1989). "Model studies of pressuremeter testing in soft rock." ASTM Geotechnical Testing Journal, 12(2).

Hughes, J., Wroth, C. and Windle, D. (1977). "Pressuremeter tests in sands." Géotechnique, 27(4), 455-477.

Hughes, J. M. O., Jefferies, M. G. and Morris, D. L. (1984). "Self-bored pressuremeter testing in the arctic offshore." Proceedings of the Offshore Technology Conference, Offshore Technology Conference, Houston, Texas, 255-264.

Isik, N. S., Ulusay, R. and Doyuran, V. (2008). "Deformation modulus of heavily jointed-sheared and blocky greywackes by pressuremeter tests: numerical, experimental and empirical assessments." Engineering Geology, 101(1), 269-82.

Jang, I. S., Chung, C., Kim, M. M. and Cho, S. M. (2003). "Numerical assessment on the consolidation characteristics of clays from strain holding, self-boring pressuremeter test." Computers and Geotechnics, 30(1), 121-40.

Janin, J. P. et. al., (2015). "Numerical back-analysis of the southern toulon tunnel measurements: a comparison of 3D and 2D approaches." Engineering Geology, 195(1), 45-52.

Ladanyi, B. (1963). "Evaluation of pressuremeter tests in granular soils." Proc. 2nd Panamerican Conf. on Soil Mech and Found. Engrg., 3-20.

Marsland, A. and Randolph, M. (1977). "Comparisons of the results from pressuremeter tests and large in situ plate tests in London Clay." Géotechnique, 27(2), 217-243.

Nordal, S. (1999). "Present of Plaxis." Beyond 2000 in Computational Geotechnics, Balkerma, Rotterdam, 45-54.

Palmer, A. C. (1972). "Undrained plane-strain expansion of a cylindrical cavity in clay: a simple interpretation of the pressuremeter test." Geotechnique, 22(3), 451-7.

Plaxis (2013). Reference manual, Plaxis, Delft University of Technology, Delft, Netherlands.

Schanz, T., Vermeer, P. A. and Bonnier, P. G. 1999, 'The hardening soil model: formulation and verification', in Beyond 2000 in Computational Geotechnics, Balkema, Rotterdam, 281-296.

Vesic, A. S. (1972). "Expansion of cavities in infinite soil mass." Journal of the Soil Mechanics and Foundations Division, 98(3), 265-90.

Wroth, C. P. (1982). "British experience with the self-boring pressuremeter." Proceedings of Symposium on the Pressuremeter and its Marine Applications, Paris, 143-164.

Wroth, C. P. and Hughes, J. M. O. (1973). "An instrument for the in-situ measurement of the properties of soft clays." Proc. 8th Int. Conf. SMFE, Moscow, Russia, 487-494.

Yu, H. S. (1994). "State parameter from self-boring pressuremeter tests in sand." Journal of Geotechnical Engineering, 120(12), 2118-35.

Yu, H. S. (2000). Cavity Expansion in Geomechanics, Springer Science+Business Media, B.V., Dordrecht.